

Propagation-invariant vectorial Bessel beams obtained by use of quantized Pancharatnam–Berry phase optical elements

Avi Niv, Gabriel Biener, Vladimir Kleiner, and Erez Hasman

Optical Engineering Laboratory, Faculty of Mechanical Engineering, Technion—Israel Institute of Technology, Haifa 32000, Israel

Received August 18, 2003

Propagation-invariant vectorial Bessel beams with linearly polarized axial symmetry based on quantized Pancharatnam–Berry phase optical elements are described. The geometric phase is formed through the use of discrete computer-generated space-variant subwavelength dielectric gratings. We have verified the polarization properties of our elements for laser radiation at 10.6- μm wavelength and also demonstrated propagation-invariant, controlled rotation of a propeller-shaped intensity pattern through the simple rotation of a polarizer. © 2004 Optical Society of America

OCIS codes: 260.5430, 050.2770, 050.1960, 230.5440.

Propagation-invariant scalar fields have been extensively studied, both theoretically and experimentally, since they were proposed by Durnin *et al.*¹ These fields were employed in applications such as optical tweezers and for transport and guiding of microspheres.² Although there has recently been considerable theoretical interest in propagation-invariant vectorial beams,³ experimental studies of such beams have remained somewhat limited.^{4,5} One of the most interesting types of propagation-invariant vectorial beam is the linearly polarized axially symmetric beam (LPASB).^{3,4,6} These vectorial beams are characterized by their polarization orientation, $\psi(\omega) = m\omega + \psi_0$, where m is the polarization order, ω is the azimuthal angle of the polar coordinates, and ψ_0 is the initial polarization orientation for $\omega = 0$. LPASBs can be formed by interferometric techniques, by the intracavity summation of two orthogonally polarized TEM₀₁ modes,⁷ or by liquid-crystal devices.⁸ However, all these methods are somewhat cumbersome, are unstable, or have low efficiency. We recently demonstrated the use of continuous space-variant subwavelength gratings for the formation of LPASBs.⁶ However, applying the constraint to continuity of the subwavelength grating led to a variation of the local period. As a result, the elements became limited in their physical dimensions, and optimization of the photolithographic process was complicated.

In this Letter we propose the formation of propagation-invariant vectorial Bessel beams by use of quantized Pancharatnam–Berry phase optical elements (QPBOEs) followed by an axicon. QPBOEs utilize the geometric phase that accompanies space-variant polarization manipulations to achieve a desired phase modification.⁹ To test our approach we formed QPBOEs with different polarization orders as computer-generated space-variant subwavelength gratings upon GaAs wafers for use with 10.6- μm laser radiation. By discretely controlling the local grating orientation, which has uniform periodicity, we could form complex vectorial fields with elements of unlimited physical dimensions. We experimentally determined the optical performance of the elements by measuring the polarization distribution of the emerging beam through the QPBOE, verifying the high quality of LPASBs. Subsequently,

propagation-invariant vectorial Bessel beams were achieved by insertion of an axicon after the QPBOEs. Finally, the resultant beams were transmitted through a polarizer that produced a unique propagation-invariant scalar beam. This beam has a propeller-shaped intensity pattern that can be rotated by simple rotation of the polarizer. We therefore have demonstrated the formation of a vectorial Bessel beam by using simple, lightweight thin elements and exploited that beam to perform a controlled rotation of a propeller-shaped intensity pattern that can be suitable for optical tweezers.¹⁰

The Jones vector of a LPASB is given by $|P_m\rangle = [\exp(im\omega)|R\rangle + \exp(-im\omega)|L\rangle]/\sqrt{2}$, where $|R\rangle = (1, -i)^T/\sqrt{2}$ and $|L\rangle = (1, i)^T/\sqrt{2}$ are the helical basis unit vectors and the superscript T denotes a vector transposition. The $|P_m\rangle$ state represents the linearly polarized beam whose polarization azimuthal angle is given by $\psi = m\omega$ (we chose the reference axis such that $\psi = 0$ at $\omega = 0$). Note that, because the azimuthal angle is a π -modulo function, the polarization state repeats itself $2m$ times for each trip about the beam axis. Propagation of the $|P_m\rangle$ state when it is transmitted through an axicon can be approximated by the stationary phase method⁴ to yield

$$\begin{aligned} |B_m\rangle &= K_z[f(r)|P_m\rangle] \\ &\cong (\pi\alpha\sqrt{z/\lambda})\exp\{ik[(1 - \alpha^2/2)z + r^2/2z - \lambda/8]\} \\ &\quad \times (-i)^m J_m(kar)|P_m\rangle, \end{aligned}$$

where K_z is the Fresnel free-space propagation operator for propagation distance z , r is the radius of the polar coordinates, k is the wave number, and J_m is the m th-order Bessel function of the first kind. In this case the axicon phase function is paraxially approximated by $f(r) = \exp(-ikar)$, where $\alpha = \theta(n - 1)$ and θ and n are the inclination angle and the refractive index of the axicon, respectively. This paraxial calculation confirms propagation invariance of the polarization state as well as the Bessel intensity distribution, except for a linear growth function of z that one can remove by apodizing the incoming intensity.¹¹ For this vectorial Bessel beam the intensity profile is determined by m , the polarization order of the original

LPASB, whereas the local polarization state is unchanged by the axicon.

QPBOEs are considered constant retardation wave plates for which the fast axes are changed along the length of the elements. It is convenient to form such space-varying wave plates by use of subwavelength gratings. When the period of a periodic structure is smaller than the incident wavelength, only the zero order is a propagating order, and all other orders are evanescent. The subwavelength periodic structure thereby behaves as a uniaxial crystal with the optical axes parallel and perpendicular to the subwavelength grooves.⁹ Therefore, by fabrication of a constant-period subwavelength structure for which the orientation of the subwavelength grooves is changed along the length of the element, space-variant wave plates are obtained. These gratings are conveniently described by a space-varying Jones matrix $\mathbf{T}(r, \omega) = \mathbf{R}^{-1}[\theta(r, \omega)]\mathbf{W}\mathbf{R}[\theta(r, \omega)]$. In this case, $\mathbf{R}(\theta)$ is a two-dimensional rotation matrix and $\theta(r, \omega)$ is the local orientation of the grating. \mathbf{W} is the Jones matrix of a perfect retarder and represents the local behavior of the grating. Choosing grating parameters to achieve a local retardation of π rad and illuminating the element with linearly polarized light result in a Jones vector of the form

$$|E_{\text{out}}\rangle = \frac{1}{\sqrt{2}} \exp[i2\theta(r, \omega)]|R\rangle + \frac{1}{\sqrt{2}} \exp[-i2\theta(r, \omega)]|L\rangle.$$

The $|E_{\text{out}}\rangle$ state comprises two scalar waves of orthogonal circular polarization. The phase of each scalar component results from manipulation of the space-variant polarization state and therefore is geometric in nature. Selecting a local subwavelength groove orientation such as $\theta = m\omega/2$ results in a QPBOE with the desired $|P_m\rangle$ state when the element is illuminated with linearly polarized light. In our approach, the groove orientation is discretely approximated by $\theta(r, \omega)|_{\text{mod } \pi} = F_N(m\omega)/2$, where $F_N(x)$ is a step function that has discrete steps of $2\pi/N$. In this case, N indicates the number of quantized levels.⁹

To achieve such QPBOEs we formed four chrome masks by use of high-resolution laser lithography for $m = 1, 2, 3, 4$. We used a $2\text{-}\mu\text{m}$ subwavelength grating period and $N = 16$ quantized levels to form masks 1 cm in diameter. Magnified geometries of the masks are given in Fig. 1(a). It was previously shown that 16-level QPBOEs diffract more than 98% of the intensity into the first order.⁹ Note that the area in the center of the mask where the pattern is distorted is less than $10\text{ }\mu\text{m}$ in diameter and can therefore be disregarded. The patterns were transferred by contact lithography to $500\text{-}\mu\text{m}$ -thick GaAs wafers (refractive index, 3.27) onto which a 200-nm -thick layer of SiN_x had previously been deposited. The SiN_x deposition was performed by plasma-enhanced chemical vapor deposition at 900 mTorr and $300\text{ }^\circ\text{C}$. At this stage, adhesion of a 70-nm Ni layer was used for the lift-off process. Next, the SiN_x layer was etched through the Ni stripes, which served as a mask. Reactive ion etch-

ing was performed for 30 s at room temperature with CF_4 and O_2 at gas flow rates of 35 and 15 SCCM, respectively, where SCCM denotes cubic centimeters per minute at STP, and at a pressure of 80 mTorr . The GaAs was etched by electron cyclotron resonance, with the etched SiN_x layer serving as a mask. The conditions for electron cyclotron resonance were 20 SCCM of Cl_2 , 5 SCCM of Ar, 75 W of rf power, 600 W of microwave power, and $100\text{ }^\circ\text{C}$. The remaining SiN_x was removed with HF acid. The result was a space-variant grating of $5\text{-}\mu\text{m}$ nominal depth with a 5% standard deviation (STD). At this stage an antireflection coating was provided to the backside of the elements to finish forming the desired QPBOEs. Scanning-electron microscope images of the elements' central sections are given in Fig. 1(b). A high aspect ratio ($\sim 1/5$) and grooves of rectangular shape were achieved.

Following the fabrication, the elements were illuminated with a linearly polarized plane wave at a wavelength of $10.6\text{ }\mu\text{m}$ from a CO_2 laser. The local azimuthal angle was observed by insertion of a polarizer directly behind the QPBOEs. The resultant intensities are depicted in Fig. 2(a). Note that a specific azimuthal angle returns $2m$ times within each trip about the beam's axis. We measured the normalized Stokes parameters (S_1, S_2, S_3) of the

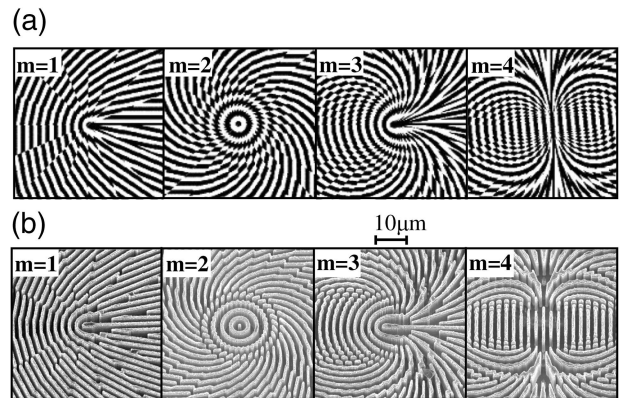


Fig. 1. (a) Magnified geometries of the masks for various polarization orders. (b) Scanning-electron microscope images of the central parts of the corresponding elements.

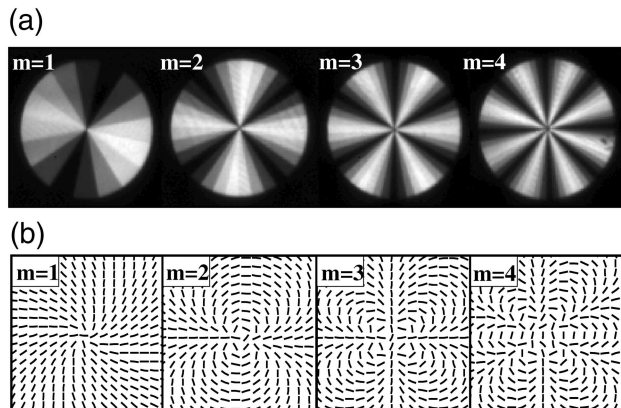


Fig. 2. (a) Experimental intensity distributions, directly after the elements, for beams emerging from a linear polarizer for four polarization orders. (b) Measured local azimuthal angles of the beams.

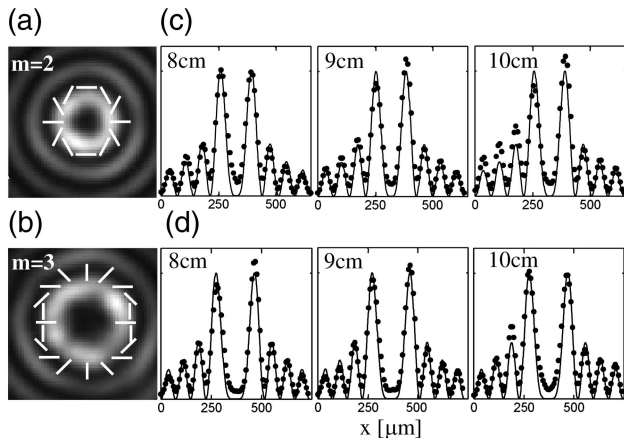


Fig. 3. Intensity distributions at 8 cm beyond the axicon for (a) $m = 2$ and (b) $m = 3$. The strips arranged along the circumference of a beam illustrate the local azimuthal angles. (c), (d) Experimental (filled circles) and theoretical (solid curves) intensity cross sections for $m = 2$ and $m = 3$, respectively, at 8, 9, and 10 cm beyond the axicon.

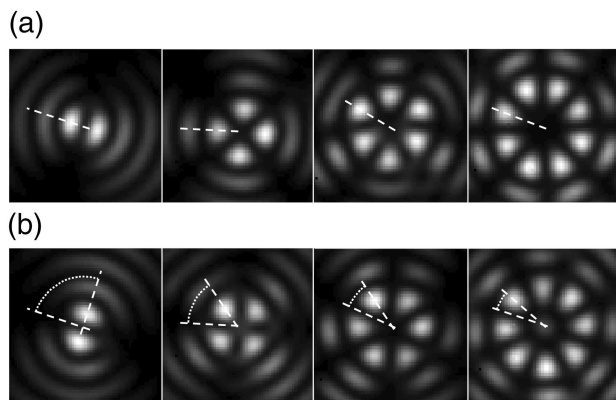


Fig. 4. (a) Propeller-shaped intensity patterns of the emerging beams from the QPBOEs followed by an axicon and a polarizer for four polarization orders, $m = 1, 2, 3, 4$, from left to right. (b) Controlled rotation of the propeller-shaped intensities by rotation of the polarizer by 90° ; dashed lines and dotted curves, rotation angles of the patterns.

emerging beams in the near field.⁶ Figure 2(b) shows the measured local azimuthal angles of the beams calculated by $\psi = \tan^{-1}(S_2/S_1)/2$. The typical STD of ψ from the desired value was found to be 1.5° . Note that the measured azimuthal angle distributions are in good agreement with the desired values given by $\psi = m\omega$. The local ellipticity was calculated as $\chi = \sin^{-1}(S_3)/2$, resulting in a typical average value of 4.3° with a typical STD of 4° . The deviation of the ellipticity from its desired zero value is related to errors in the nominal etching depth, whereas its relatively large STD results from nonuniformity of the etching depth. The azimuthal angle is determined by the groove's orientation and is, therefore, relatively accurate. The ability to create high-quality LPASBs by use of QPBOEs is therefore demonstrated. We obtained propagation-invariant vectorial beams by inserting a ZnSe axicon ($\theta = 3^\circ$, $n = 2.4$) following the QPBOEs.

Figures 3(a) and 3(b) show the intensities at 8 cm beyond the axicon for beams of polarization orders $m = 2, 3$, respectively. The white stripes arranged along the circumferences of the beams illustrate the local azimuthal angles. Figures 3(c) and 3(d) show the theoretical and experimental normalized intensity cross sections for $m = 2, 3$, respectively, at 8, 9, and 10 cm beyond the axicon. The theoretical prediction is given by the $|B_m\rangle$ state. We also measured a typical STD of the azimuthal angles from the desired values over the propagation distances to be 4.7° and a typical ellipticity of 5.5° with a STD of 5.7° . We thereby experimentally confirmed the formation of propagation-invariant vectorial Bessel beams.

Finally, we demonstrated the ability to achieve controlled rotation of the intensity pattern by inserting a polarizer behind the axicon. It can be shown, again by use of a stationary phase approximation, that transmittance of propagation-invariant LPASBs through a polarizer results in an amplitude of $\propto J_m(kar)\cos(m\omega)$. This beam is propagation invariant, with a propeller-shaped intensity pattern given by $I \propto J_m^2(kar)[1 + \cos(2m\omega)]$. These propeller-shaped intensities are depicted in Fig. 4(a). As expected, each propeller comprises $2m$ fringes. If the polarizer is rotated by an angle ω_0 , the fringes rotate by an angle ω_0/m . This behavior is demonstrated in Fig. 4(b), for which the polarizer has been rotated by 90° . The dashed lines and dotted curves indicate the resultant rotation of the propellers. It is evident that rotations of 90° , 45° , 30° , and 22.5° were obtained for $m = 1, 2, 3, 4$, respectively.

We have therefore demonstrated the formation of LPASBs by use of thin, lightweight elements and have shown that these beams become propagation invariant when they are transmitted through an axicon.

E. Hasman's e-mail address is mehasman@tx.technion.ac.il.

References

1. J. Durnin, J. Miceli, Jr., and J. H. Eberly, Phys. Rev. Lett. **58**, 1499 (1987).
2. V. Garcés-Chávez, D. McGloin, H. Melville, W. Sibbett, and K. Dholakia, Nature **419**, 145 (2002).
3. J. Tervo and J. Turunen, Opt. Commun. **192**, 13 (2001).
4. P. Pääkkönen, J. Tervo, P. Vehimaa, J. Turunen, and F. Gori, Opt. Express **10**, 949 (2002), <http://www.opticsexpress.org>.
5. Z. Bomzon, A. Niv, G. Biener, V. Kleiner, and E. Hasman, Appl. Phys. Lett. **80**, 3685 (2002).
6. A. Niv, G. Biener, V. Kleiner, and E. Hasman, Opt. Lett. **28**, 510 (2003).
7. R. Oron, S. Bilt, N. Davidson, A. A. Freisem, Z. Bomzon, and E. Hasman, Appl. Phys. Lett. **77**, 3322 (2000).
8. J. A. Davis, D. E. McNamara, D. M. Cottrell, and T. Sonehara, Appl. Opt. **39**, 1594 (2000).
9. E. Hasman, V. Kleiner, G. Biener, and A. Niv, Appl. Phys. Lett. **82**, 328 (2003).
10. M. P. MacDonald, L. Paterson, K. Volke-Sepulveda, J. Arlt, W. Sibbett, and K. Dholakia, Science **296**, 1101 (2002).
11. N. Davidson, A. A. Friesem, and E. Hasman, Opt. Commun. **88**, 326 (1992).